Rev. Roum. Sci. Techn.– Électrotechn. et Énerg.
Vol. **68**, 2, pp. 127–131, Bucarest, 2023

METAMATERIAL INSPIRED SPLIT RING RESONATOR ACCOMPLISHED MULTIBAND ANTENNA FOR 5G AND OTHER WIRELESS APPLICATIONS

PANKAJ JHA[1], ANUBHAV KUMAR[2], NAVNEET SHARMA[3]

Keywords: Multiband antenna; Metamaterial inspired antenna; Defected ground structure (DGS); Split ring resonator (SRR); Gain enhancement.

A multiband antenna is proposed in this paper, accomplished with a split ring resonator (SRR) in the ground plane for portable and wireless applications. The rectangular radiator is unified with a semi-circular stub improving the impedance matching in the antenna. Further, the radiator creates an optimized rectangular slot to obtain the multiband operation. The SRR in the ground plane demonstrates the metamaterial (MTM) characteristics that significantly improve the 10 dB impedance bandwidths (IBW) and enhance realized gain in the multi-band antenna. The proposed antenna is procuring the five 10 dB IBW, which can be prominent for RADAR (2.96 GHz - 3.06 GHz), 5G (3.92 GHz - 4.32 GHz and 4.64 GHz - 5.04 GHz), WLAN (5.32 GHz - 5.64 GHz) and ISM band (5.7 GHz - 6 GHz) applications. The gain enhancement is obtained in all operating bands of the antenna, and a maximum 5.24 dB gain is achieved at a 4.14 GHz frequency.

1. INTRODUCTION

A wireless communication system demands high-performance microstrip antennas to fulfill the requirements of an existing communication system where the bandwidth and gain are two important parameters. Several applications per allotted band can be executed with the single antenna element through the multiband antenna, making it prevalent. Communication signals can be effectively transmitted and received by a high-gain antenna [1], but achieving the high gain in the compact antenna is not straightforward. Keeping this contest in mind, several practices are being used for the enhancement of antenna gain, which majorly include artificial magnetic conductor (AMC) [2–4], defective ground structure (DGS) [5-7], metamaterial [8–12], frequency selective surface (FSS) [13–17].

AMC and FSS control the grating lobes of the antenna and enhance the overall gain, but the antenna size is compromised. In contrast, DGS increases the complexity of the antenna for practical applications.

In [2], AMC technology increases the gain of a multi-band antenna where the AMC is placed below the antenna, and gain enhancement depends upon the reflection phase angle. In [3], the second-order rectangular loop fractal AMC is placed parallel to the ground plane in a wideband antenna for gain enhancement. In [4], a modified circular loop AMC loaded on the co-planar waveguide (CPW) antenna effectively reflected the grating lobes and worked as a reflector, increasing the antenna gain. In [5], conventional electromagnetic bandgap (EBG) technology is used with the defected ground, significantly enhancing the antenna's gain.

In [6], dipole antenna gain is increased by split ring resonator (SRR) metamaterial unit cell, where metamaterial (MTM) characteristics of SRR are responsible for gain enhancement. In [7], the dielectric superstrate enhances the antenna's gain, where the radius of holes in the superstrate adjusts the effective permittivity. In [8], a metamaterial Jerusalem cross-unit cell based on zero refractive indexes is used for gain enrichment of patch antenna with single and double-layer superstrate. In [9], a metamaterial unit cell in the ground plane as a DGS is accomplished, enhancing the gain of a dual-band antenna.
In [10], two hexagonal metamaterial cells are placed behind the antenna having double negative (DNG) MTM properties, influencing both antenna bands' gain. In [11], double-sided FSS with a circular-shaped structure is used for gain enhancement of a millimeter wave antenna where FSS is positioned above the antenna to work as a passband, improving the antenna's radiation pattern. In [12], modified SRR structured FSS works as a passband, enhancing the CPW-fed antenna's gain. In [13], FSS is designed using four asymmetric rectangular conducting elements in one unit cell accomplished with circular slots for the UWB antenna. In [14], a dual-layer FSS is discussed for gain enhancement of the antenna operating at the ISM band. In [15], a two-layer FSS is developed for an umbrella-shaped antenna where the UWB antenna achieved up to 4 dB gain enhancement accomplished with an air gap between the arrays. In [16], four interconnected square loop metallic patches are used to design an FSS demonstrating the stopband characteristics in the entire operating band. In [17], two layers of thin FSS are designed accomplished with cross-shape and circular-shape structures in the top and bottom layers. In [18], a polygon-shaped multiband antenna is designed to exhibit the MTM characteristics in all operating bands.

The proposed work is delineated to cover the sub-6 GHz frequency band with the multiband operation and improved gain. The proposed antenna uses the SRR-based ground with a simple structure to enhance the antenna's 10 dB impedance bandwidth (IBW) and gain. MTM behavior of SRR is responsible for the higher gain enhancement in the proposed work compared to recent results, as illustrated in table 1. The obtained bands of the proposed antenna can be used in portable devices, radar applications, 5G, WLAN, and ISM band applications.

2. ANTENNA EVOLUTION AND DESIGN

The proposed antenna is designed with $0.972\lambda_g \times 0.972\lambda_g \times 0.0259\ \lambda_g$ dimensions where λ_g is the center frequency, and

[1] IIMT College of Engineering, Greater Noida, GB Nagar, UP, India, pankaj.maahi@gmail.com
[2] Raj Kumar Goel Institute of Technology and Management, Ghaziabad, UP, India, rajput.anubhav@gmail.com
[3] ABES Engineering College, Ghaziabad, UP, India, navneet1979@gmail.com

it can be calculated from

$$\lambda_g = \lambda_0/(\sqrt{\varepsilon_e}), \quad (1)$$

$$\varepsilon_e = (\varepsilon_r+1)/2, \quad (2)$$

where λ_0 represents a wavelength of lower operating frequency.

The layout of the antenna is depicted in Fig. 1 (a), and its fabricated prototype is depicted in Fig. 1 (b) and (c). The FR4 substrate designs the MTM-inspired multiband antenna while the dielectric constant is 4.4, constant in the full frequency band. The pertaining dimensions of the antenna geometry are W1 = 60 mm, L1 = 60 mm, W2 = 2 mm, L2 = 15 mm, W3 = 20 mm, L3 = 25 mm, W4 = 3 mm, L4 = 7.75 mm, L5 = 40 mm, L6 = 5 mm, the radius of semicircle W5 = 15 mm and W6 = 2 mm.

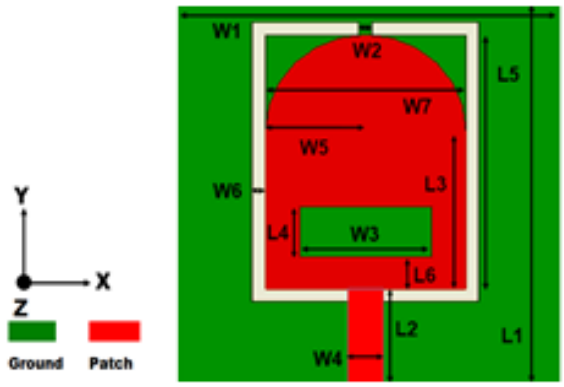

(a)

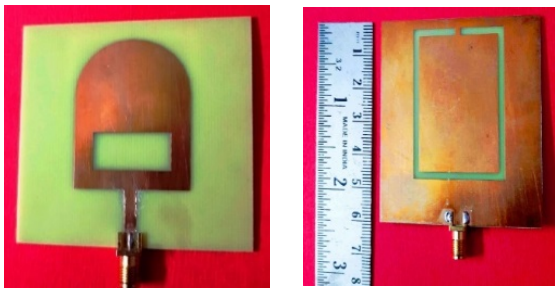

(b) (c)

Fig. 1 – (a) Dimensions of the proposed antenna (b) & (c) Front and bottom plane of the experimental antenna. Fig. 1d is missing.

Three progressive steps are used to optimize the dimensions of the finalized antenna, as painted in Fig. 2 (a). In Step (S) 1, a microstrip antenna is designed using a rectangular radiator unified with a semi-circular stub with full ground. The rectangular radiator dimensions are 30 mm x 25 mm combined with a 15 mm semi-circle. Microstrip feed of length 15 mm and width 3 mm is considered in the antenna to achieve impedance matching of 50 Ω. The microstrip antenna exhibits a 10 dB impedance bandwidth from 3.7 to 3.75 GHz. In S-2, a rectangular slot is introduced in the radiator, which amends the surface current, resulting in an additional operating band in the antenna.

The 10 dB IBW is obtained from 4.61 to 4.8 and 5.56 to 5.67 GHz. In S-3, SRR is introduced in the ground plane, acting as a stopband up to 6 GHz frequency observed in Fig. 4,a. It alters the current directions and modifies the lumped element of the antenna, significantly improving its impedance matching. The SRR in the ground plane, owing to the MTM properties, creates the three additional operating bands in the multiband antenna. This modification also controls the grating lobes generated by the antenna, resulting in an overall gain enhancement in all the obtained bands. The antenna's final 10 dB IBW varies from 2.96 to 3.06 GHz, 3.92 to 4.32 GHz, 4.64 to 5.04 GHz, 5.32 to 5.64 GHz, and 5.7 to 6 GHz frequency. The simulated scattering parameter $|S_{11}|$ and gain of the antenna evolution steps are depicted in Fig. 2,b,c. The current density distribution at lower and upper resonant frequencies (3 GHz and 5.8 GHz) is shown in Fig. 2,d.

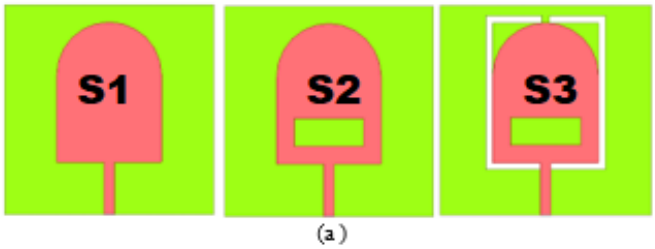

(a)

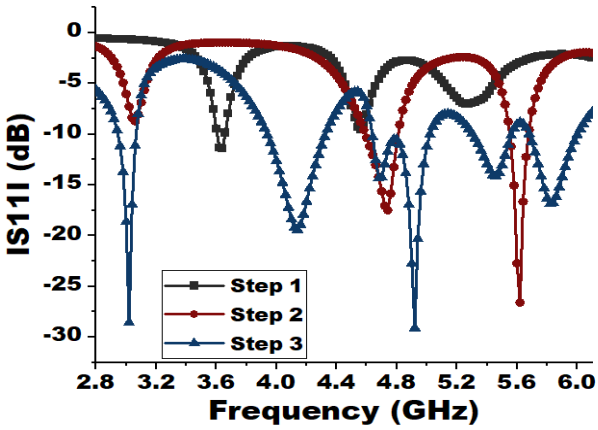

(b)

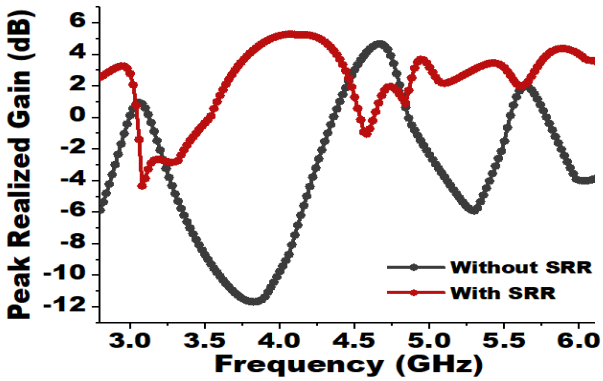

(c)

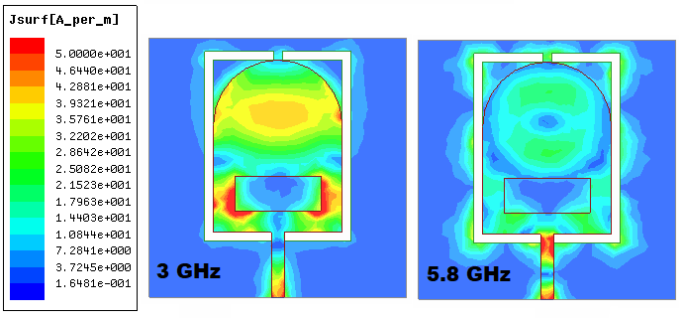

(d)

Fig. 2 – (a) Antenna evolution steps, (b) The simulated |S11| of antenna steps, (c) Realized gain (dB) with and without SRR, (d) distribution of surface electric field intensity at 3 & 5.8 GHz frequency.

3. PARAMETRIC ANALYSIS

To validate the optimized performance of the proposed antenna, its parametric variations are analyzed with length L4, L6, and width W2, W3. The parametric length (L4) has been varied from 3.75 mm to 11.75 mm with a 2 mm step size. The optimum value of L4 is 7.75 mm, as depicted in Fig. 3 (a).

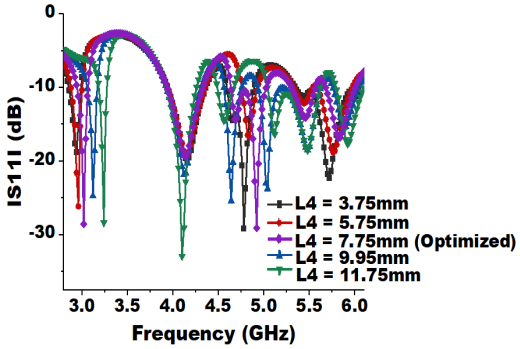

(a)

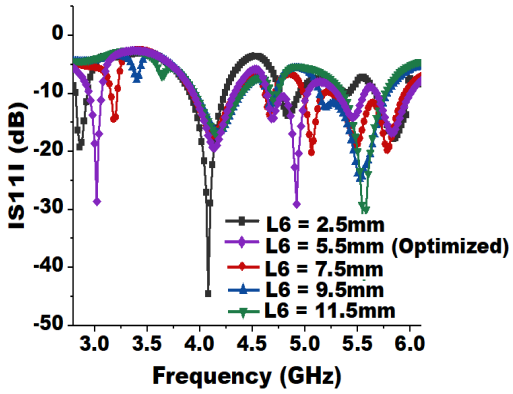

(b)

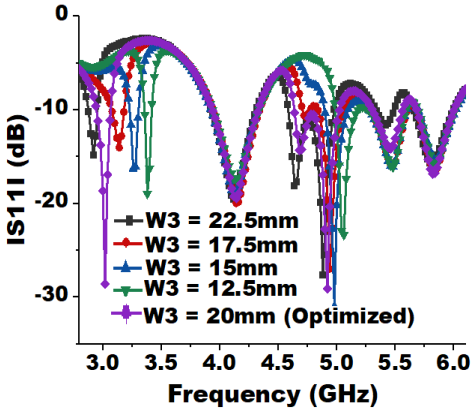

(c)

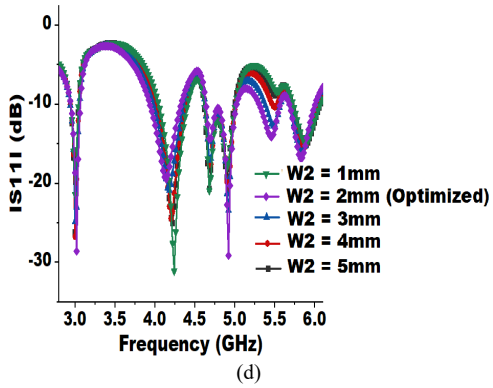

(d)

Fig. 3 – Parametric changes of the proposed antenna dimensions (a) Obtained |S11| by varying the L4, (b) Obtained |S11| by varying L6, (c) Obtained |S11| by varying W3, and (d) Obtained |S11| by varying W2.

The length of L6 is varied from 2.5 mm to 11.5 mm with a 2 mm step size. The resonant frequency shifts towards the higher frequency, and impedance matching, are reduced when the length of L6 increases, as illustrated in Fig. 3 (b). The optimum value of L6 is considered 5.5 mm. The width of W3 has been varied from 12.5 mm to 22.5 mm. It is observed that when the W3 increases, the lower operating frequency band shifts toward a lower frequency. The optimized value of W3 is taken as 20 mm, shown in Fig. 3 (c). The next parametric analysis is done with a split ring resonator (SRR) by changing the width of W2. The variations of these changes are illustrated in Fig. 3(d). The width of W2 is varied from 1 mm to 5 mm, and this variation affects the 5.5 GHz resonant frequency. The optimum value of W2 was achieved at 2 mm. The optimized dimension of the antenna provides five operating bands with 10 dB IBW. These bands are 2.96 - 3.06 GHz (applicable in Radar communication), 3.92 - 4.32 GHz (n77), 4.64 - 5.04 GHz (n79), 5.32 - 5.64 GHz (E-Ultra band 46) and 5.7 - 6 GHz (applicable for ISM Band).

4. ANALYSIS OF METAMATERIAL CHARACTERISTICS

The S- scattering parameters ($|S_{11}|$ – reflection and $|S_{21}|$ - transmission) of the MTM-based antenna is illustrated in Fig. 4 (a), representing the stopband characteristics. The metamaterial behavior of the ground plane is computed from the Nicolson Ross weir method from equations 3 to 7 [18] by S- parameters extracted using Floquet port and depicted in Fig. 4,b

$$\varepsilon = \frac{nr}{z}, \tag{3}$$

$$(\mu) = nr.z \tag{4}$$

where 'nr' represents the refractive index as given in eq. (3)

$$(nr) = \frac{1}{k_0 L}\{[\mathrm{Im}[\mathrm{In}(A)] + 2m\pi] + j\mathrm{Re}[\mathrm{In}(A)]\}, \tag{5}$$

where z = Impedance and A= Absorptivity of meta-material. Both "z" and "A" can be evaluated by

$$(z) = \pm\sqrt{\frac{(1+S_{11})^2 - S_{21}^2}{(1-S_{11})^2 - S_{21}^2}} \tag{6}$$

$$(A) = \frac{S_{21}}{1 - S_{21}\frac{z-1}{z+1}}. \tag{7}$$

According to the extracted result of permittivity and permeability, it is observed that permittivity is close to zero (ENZ) in the antenna operating band from 2.96 to 3.06 GHz and 4.64 to 5.04 GHz. In contrast, permittivity is negative from 3.92 to 4.32 GHz and 5.32 to 5.64 GHz. Permittivity and permeability are negative (DNG) from 5.7 GHz to 6 GHz in the operating band. Metamaterial properties exhibited by the SRR ground also enhance the antenna performance regarding impedance matching and gain. 3.02 GHz and 4.14 GHz resonant frequencies are achieved due to the negative permittivity. The permittivity and permeability are close to zero at 4.96 GHz, whereas negative permeability is observed for 5.4 GHz and 5.8 GHz frequencies. The minimum gain is achieved on 3.2 GHz and 4.5 GHz frequencies where permeability and permittivity have maximum positive values; however, the maximum gain is achieved in the multiband antenna at that frequency where the permittivity value is the minimum. As per the above observations, it can be concluded that the proposed antenna's gain and operating bands are closely related to the metamaterial characteristics of SRR based ground plane of the antenna.

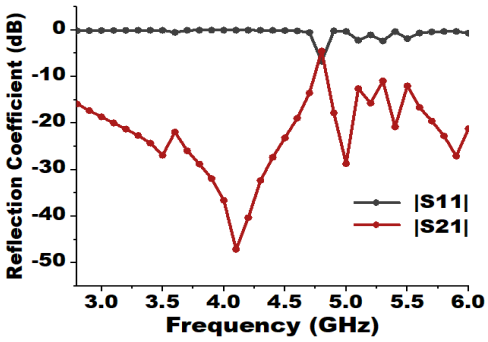

(a)

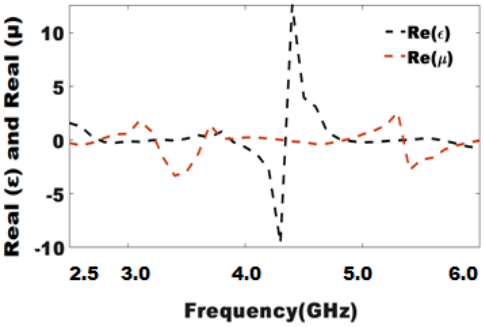

(b)

Fig. 4 – (a) Ground plane Reflection coefficient and (b) Extracted Metamaterial property based on the real value of permittivity (ε) and permeability (μ).

5. RESULTS AND DISCUSSION

The Ansys HFSS-13 simulator designs the proposed multiband antenna, and for the experimental measurements, a vector network analyzer model Anritsu MS2025 is utilized. The simulated and measured $|S_{11}|$ are close to each other with minor variations due to the soldering effect, as depicted in Fig. 5,a.

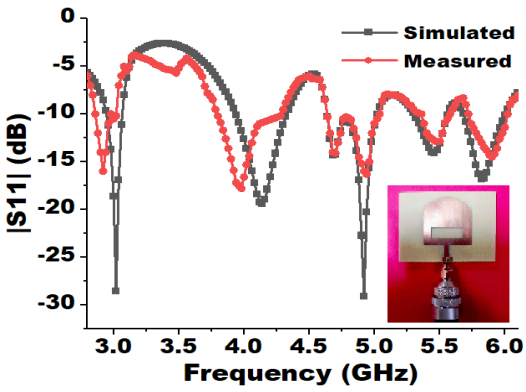

(a)

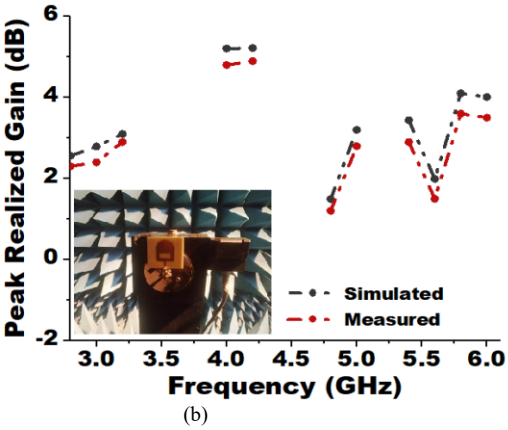

(b)

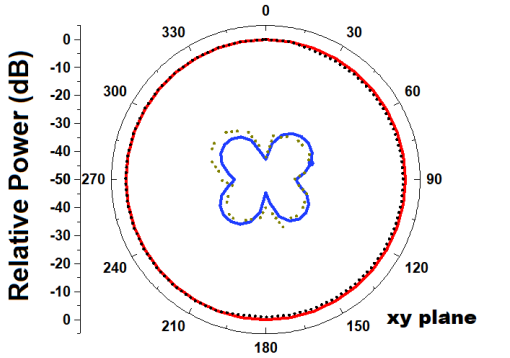

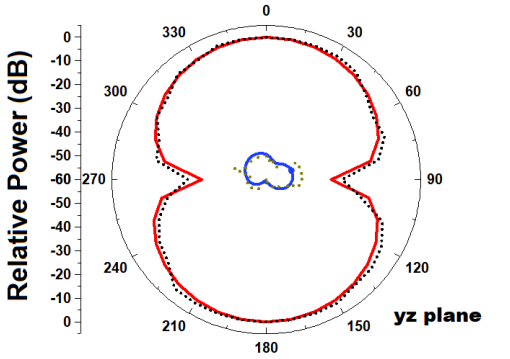

(c)

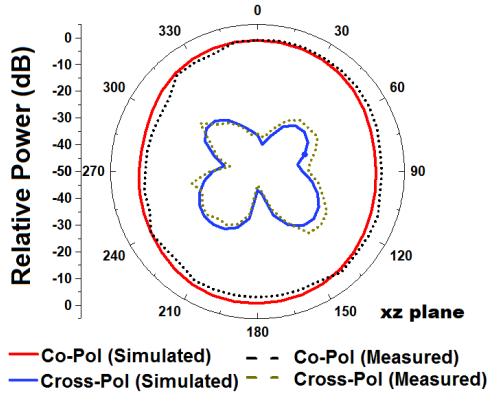

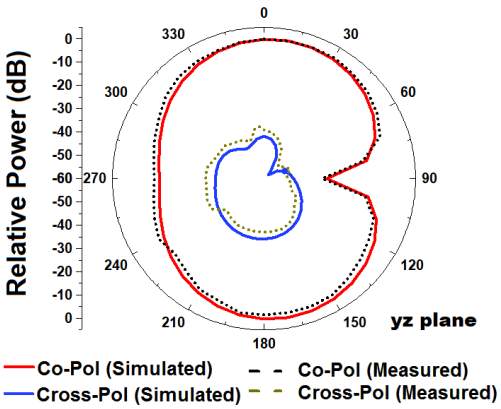

(d)

Fig. 5 (a) and (b) Comparison of experimental study and simulator |S11| and realized gain (dB) (c) Far-field patterns at 3 GHz (d) 5.8 GHz in xz and yz plane of the multiband antenna.

The far-field analysis is carried out in an anechoic chamber, and the maximum realized gain of the antenna is observed at 5.24 dB at 4.14 GHz frequency. The measured gain results have less than 0.5 dB shift compared to the simulated values,

as depicted in Fig. 5,b. The far-field analysis in the xz and yz planes is illustrated in Fig. 5,c,d at 3 GHz and 5.8 GHz frequencies. In the normalized pattern, the difference between the co and cross-polarization plane is more than 20 dB in the broadside direction, which assures a stable radiation pattern of the antenna. A comparative study against recent literature is provided in Table 1, revealing that the proposed antenna achieves multiple operating bands with an enhanced gain.

6. **CONCLUSION**

The proposed antenna represents a very good solution to the current requirements of wireless communication systems because it can cover multiple operating bands with a single antenna element. The rectangular and semicircle planes are radiators in which a rectangular slot increases impedance matching. The SRR based on a metamaterial property is accomplished in the ground plane to improve the operating bandwidth and gain effectively. The antenna covers five frequency bands that can be prominent for portable devices, Radar, 5G communications, WLAN, and ISM band applications.

Received on 28 October 2022

REFERENCES

1. A. Angeliki, M. Haardt. *Smart antenna technologies for future wireless systems: trends and challenges*, IEEE Communications Magazine, **42**, *9,* p. 90 (2004).
2. A. Ghosh et al., *Gain enhancement of triple-band patch antenna by using triple-band artificial magnetic conductor*, IET Microwaves, Antennas & Propagation, **12**, *8*, p. 1400 (2018).
3. Z., Binzhen, P. Yao, J. Duan, *Gain-enhanced antenna backed with the fractal artificial magnetic conductor*, IET Microwaves, Antennas & Propagation, **12**, *9*, p. 1457 (2018).
4. K.N. Paracha et al., *A dual-band stub-loaded AMC design for the gain enhancement of a planar monopole antenna*, Microwave and Optical Technology Letters, **60**, *9*, pp. 2108–2112 (2018).
5. S. Dhawan, A. Thakur, V.M. Srivastava, *Miniaturization and gain enhancement of microstrip patch antenna using defective ground with EBG*, Journal of Communication, **13**, *12*, p. 730 (2018).
6. G.K. Das, R. Dutta, D. Mitra, M. Mitra, *Gain enhancement of planar dipole antenna using grounded metamaterial,* Progress in Electromagnetics Research Letters, **87**, pp. 123–130 (2019).
7. J.H Kim, A. Chi-Hyung, B. Jin-Kyu, *Antenna gain enhancement using a holey superstrate*, IEEE Transactions on Antennas and Propagation, **64**, *3*, pp. 1164–1167 (2016).
8. M. Bouzouad et al., *Gain enhancement with near-zero-index metamaterial superstrate*, Applied Physics A, **121**, *3*, pp. 1075–1080 (2015).
9. R. Sourav, U. Chakraborty, *Gain enhancement of a dual-band WLAN microstrip antenna loaded with diagonal pattern metamaterials*, IET Communications, **12**, *12*, pp. 1448–1453 (2018).
10. R. Neha, N. Chattoraj, R. Mark, *Metamaterial cell inspired high gain multiband antenna for wireless applications*, AEU-International Journal of Electronics and Communications, **109**, pp. 23–30 (2019).
11. J. Min Joo et al., *Millimeter-wave microstrip patch antenna using vertically coupled split ring metaplate for gain enhancement*, Microwave, and Optical Technology Letters, **61**, *10*, pp. 2360–2365 (2019).
12. H. Zain, M.U. Khan, H.M. Cheema, *A dual-band zero-index metamaterial superstrate for concurrent antenna gain enhancement at 2.4 and 3.5 GHz*, IETE Journal of Research, **1**, pp. 2898–2908 (2020).
13. D. Priyanka, K. Mandal, *Modelling of ultra-wide stop-band frequency-selective surface to enhance the gain of a UWB antenn*a, IET Microwaves, Antennas & Propagation, **13**, *3*, pp. 269–277 (2019).
14. M.A. Belen, *Performance enhancement of a microstrip patch antenna using dual-layer frequency-selective surface for ISM band applications*, Microwave and Optical Technology Letters, **60**, *11*, pp. 2730–2734 (2018).
15. K. Surajit, A. Chatterjee, S.K. Jana, S.K. Parui, *A compact umbrella-shaped UWB antenna with gain augmentation using frequency selective surface*, Radio engineering, **27**, *2*, pp. 448–454 (2018).
16. P.G. Shankar, K. Mandal, A. Lalbakhsh, *Single-layer ultra-wide stop-band frequency selective surface using interconnected square rings*, AEU-Intern. J. of Electronics and Communications, **132**, *1*, 2021.
17. A. Bhattacharya, B. Dasgupta, R. Jyoti, *Design and analysis of ultrathin X-band frequency selective surface structure for gain enhancement of hybrid antenna*, International Journal of RF and Microwave Computer-Aided Engineering, 2020.
18. J. Pankaj, A. Kumar, A. De, R.K. Jain, *CPW-fed metamaterial inspired compact multiband antenna for LTE/5G/WLAN communication*, Frequenz, **76**, *7-8*, pp. 401–407 (2022).

Table 1

Comparative analysis with relevant multiband antenna

References	Operating bands	Centre Frequency (GHz)	The technology used for Gain improvements	Max Gain Improvement (dB)
3	Triple	3.36, 5.96, 9.09	AMC	3.77
4	Single	6	AMC	4
5	Single	4.85	AMC	2.41
6	Single	2.45	DGS + EBG	1.72
7	Single	3.5	SRR MTM	3.7
8	Single	47	MTM	2.7
9	Double	2.4, 5.15	MTM	3.69
10	Double	5.9, 9.9	MTM	4
11	Single	28	MTM	5.35
12	Double	2.5, 3.5	MTM	3.2
Proposed Work	Five	3.02, 4.14, 4.96, 5.44 & 5.8	MTM	5.4